Physics in Collision - Zeuthen, Germany, June 26-28, 2003

HARD PROCESSES IN ELECTRON-PROTON SCATTERING

Hans-Christian Schultz-Coulon
Institut für Physik, Universität Dortmund

ABSTRACT

This report summarizes some of the recent HERA results obtained by studying hard processes in ep–scattering. By resolving the structure of the proton, hard ep–reactions provide information on the parton content of the proton and may give insight into the dynamics of the exchanged parton cascade. In addition, their study offers the possibility to test the Standard Model, in particular perturbative Quantum Chromodynamics, on which the theoretical predictions on ep–scattering cross sections are generally based. Any observed deviation between the data and existing theoretical models would either indicate the need to calculate higher order contributions or hint at signs of new physics.

1 Introduction

At HERA 27.5 GeV electrons or positrons collide head on with 920 GeV protons[1], leading to a center-of-mass energy $\sqrt{s}$ of approximately 320 GeV. Due to this large center-of-mass energy the HERA facility, with its two collider experiments H1 and ZEUS, offers the possibility to probe the structure of the proton down to very small distances ($\sim 10^{-18}$ m).

For a particular *ep*–process the resolving power with which the proton structure is analyzed, is either given by the virtuality Q^2 of the exchanged photon, Z– or W–boson, or by any other hard scale, μ^2, inherent to the process studied. Apart from the investigation of inclusive deep-inelastic scattering (DIS), studies of hard *ep*–processes hence also comprise the analysis of exclusive final states, in particular jet topologies, where substantial resolving power may be provided at low Q^2 due to the choice $\mu^2 = E_T^2$, with E_T representing the transverse energy of the observed jets.

This report summarizes some of the most recent measurements obtained from analyzing inclusive DIS data (section 2) as well as some new HERA results in jet physics (section 3). In addition, section 4 is dedicated to the search for new phenomena presenting the unexpected observations of events with a high-p_t isolated lepton and missing transverse momentum and of multi-electron topologies.

2 Inclusive Deep-Inelastic Scattering

The Born cross section [1, 2] for the neutral current DIS reaction $e^{\pm}p \to e^{\pm}X$ is given by

$$\frac{d^2\sigma^{\pm}_{\rm NC}}{dx\,dQ^2} = \frac{2\pi\alpha^2}{xQ^4}\left\{Y_+(y)\,\mathcal{F}_2(x,Q^2) \mp Y_-(y)\,x\mathcal{F}_3(x,Q^2) - y^2\mathcal{F}_L(x,Q^2)\right\} \qquad (1)$$

where $Q^2 = -q^2$ is the negative four-momentum transfer squared carried by the exchanged gauge boson (γ or Z^0), x represents the Bjorken scaling variable, and $Y_\pm = 1 \pm (1-y)^2$ (with $y = Q^2/xs$) describes the helicity dependence of the electroweak interactions. The partonic structure of the proton is then contained in the generalized structure functions $\mathcal{F}_2$, $\mathcal{F}_3$ and $\mathcal{F}_L$. For unpolarized beams $\mathcal{F}_2$ and $\mathcal{F}_3$ can be written as

$$\begin{pmatrix} \mathcal{F}_2(x,Q^2) \\ x\mathcal{F}_3(x,Q^2) \end{pmatrix} = \sum_{q=\text{quarks}} x \begin{pmatrix} C_2^q(Q^2)\,[q(x,Q^2) + \bar{q}(x,Q^2)] \\ C_3^q(Q^2)\,[q(x,Q^2) - \bar{q}(x,Q^2)] \end{pmatrix}. \qquad (2)$$

[1]The proton beam energy has been increased from 820 GeV to 920 GeV after the 1997 data taking period; data recorded before 1998 are taken at a center-of-mass energy of 300 GeV.

Here, q and $\bar{q}$ are the quark densities depending on x and Q^2 alone, while the coefficient functions C_2^q and C_3^q can be expressed in terms of precisely measured electroweak parameters [2]. The longitudinal structure function $\mathcal{F}_L$ contributes only at high y and is related to the gluon content of the proton.

In contrast to neutral current interactions, for which all quark and anti-quark flavours contribute, charged current $e^-p \to \nu X$ ($e^+p \to \bar{\nu} X$) reactions probe only up-type (down-type) quarks and down-type (up-type) anti-quarks, as they are mediated by the exchange of a W^- (W^+) boson. Charged current reactions thus allow for flavour-specific investigations of the parton momentum distributions and can provide additional information on the quark content of the proton at high x and high Q^2. Since only the weak interaction contributes, the expression for the double differential charged current cross section at the Born-level [2] can be written in a somewhat simpler form than in the neutral current case:

$$\frac{d^2\sigma^{\pm}_{\rm CC}}{dx\,dQ^2} = \frac{G_F^2 M_W^4}{2\pi x}\frac{1}{(Q^2+M_W^2)^2}\tilde{\sigma}^{\pm}_{\rm CC} \quad , \tag{3}$$

with the reduced cross section $\tilde{\sigma}^{\pm}_{\rm CC}$ given by

$$\tilde{\sigma}^{+}_{\rm CC} = x\left[(\bar{u}(x,Q^2)+\bar{c}(x,Q^2)) + (1-y)^2(d(x,Q^2)+s(x,Q^2))\right] \tag{4}$$

$$\tilde{\sigma}^{-}_{\rm CC} = x\left[(u(x,Q^2)+c(x,Q^2)) + (1-y)^2(\bar{d}(x,Q^2)+\bar{s}(x,Q^2))\right] \quad . \tag{5}$$

Here u, c, d and s are the quark and $\bar{u}$, $\bar{c}$, $\bar{d}$ and $\bar{s}$ the anti-quark distributions. From these equations the sensitivity of charged current reactions to the different quark densities becomes evident; at high x, where the contribution from the sea can be neglected, e^-p scattering provides direct access to the u-quark distributions, while positron-proton collisions probe the d-quark content of the proton.

The neutral current (NC) and charged current (CC) cross sections have been measured by both the H1 [3–7] and the ZEUS [8–11] collaborations. From these measurements information on the proton structure is derived in the form of structure functions and parton distributions.

2.1 F_2–Measurements and Parton Distributions

The proton structure function $F_2 = x\sum e_q^2(q(x,Q^2)+\bar{q}(x,Q^2))$, defined as the electromagnetic contribution to $\mathcal{F}_2$, has been precisely measured by H1 and ZEUS using neutral current data. The most recent results are shown in Fig. 1 together with data from fixed target experiments. The present precision reached is of the order of 2−3%, apart from measurements at large Q^2 or at the edges of the acceptance region.

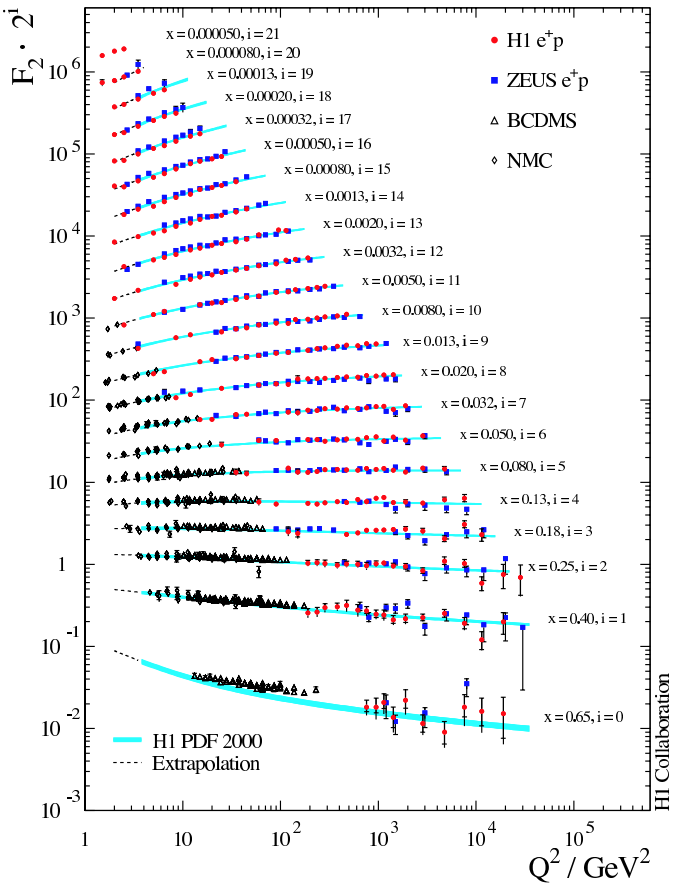

Figure 1: *The proton structure function F_2 shown as a function of Q^2 for fixed values of x. QCD fits and results from fixed target experiments are also shown.*

The data shown in Fig. 1 cover a large region in x and Q^2, clearly exhibiting the well known scaling violations of F_2 via the dependence on Q^2. In the framework of perturbative QCD these scaling violations are successfully predicted by the DGLAP equations [12], which describe the Q^2–evolution of the quark and gluon densities in the proton. At small values of x the behaviour of F_2 is dominated by quark-antiquark pair-production arising from gluon splitting and is given by $\partial F_2/\partial \ln Q^2 \sim \alpha_s \cdot xg(x)$. DGLAP based QCD fits to these data thus allow, apart from a determination of the quark content in the proton, also an extraction of the gluon density and the strong coupling constant α_s.

The most recent H1 QCD fit [5] (H1 PDF 2000 fit), shown in Fig. 1, describes the H1 and ZEUS data well over several orders of magnitude in x and Q^2. A similar fit was performed by the ZEUS collaboration [13]. Both fits are based on the same standard procedure, for which the parton distribution functions (PDF) are parametrized at a starting scale Q_0^2 and then evolved to higher Q^2 according to the next-to-leading order DGLAP equations [14]. The parameters at Q_0^2 are determined by a fit of the calculated cross section or F_2 values to the data. The QCD analyses

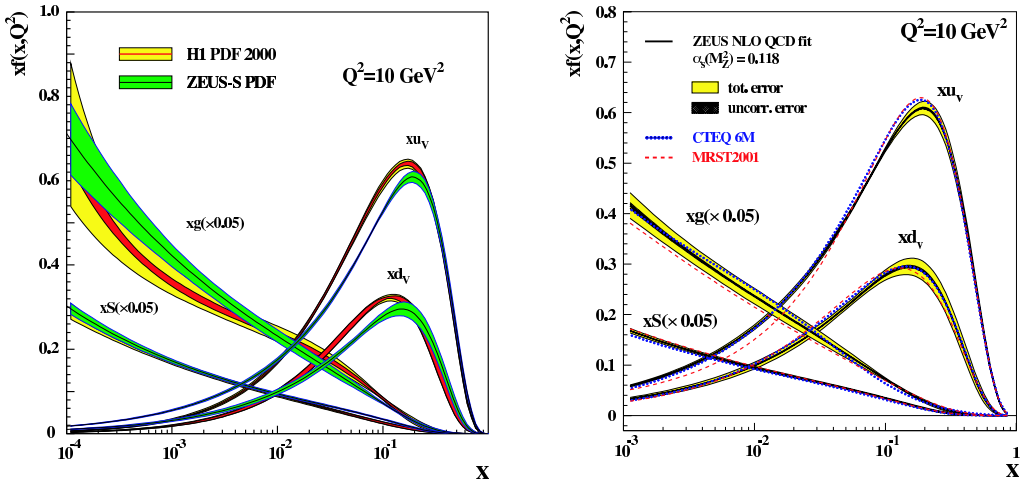

Figure 2: *(a) Comparison of PDFs obtained from the H1 PDF 2000 and the ZEUS NLO QCD fit. Shown are the valence quark distributions xu_v and xd_v, together with the gluon (xg) and sea (xS) quark densities both scaled down by a factor of 20. (b) Comparison of the ZEUS NLO QCD fit with the global analyses MRST2001 [15] and CTEQ6 [16].*

of H1 and ZEUS differ mainly by the amount of non-HERA data used, the handling of systematic errors, the parametrization at Q_0^2, and the treatment of heavy quarks.

The H1 PDF 2000 fit uses H1 neutral current (NC) and charged current (CC) data only. It determines the gluon density $g(x)$ and four up and down combinations $U = u + c$, $\bar{U} = \bar{u} + \bar{c}$, $D = d + s$ and $\bar{D} = \bar{d} + \bar{s}$ from which the valence densities $u_v - U - \bar{U}$ and $d_v = D - \bar{D}$ can be derived. In contrast, the most recent ZEUS QCD analysis [13] includes the ZEUS NC measurements together with μp and μd results from BCDMS, NMC and E665, and CCFR νFe–scattering data.

The results of these fits at $Q^2 = 10\,\mathrm{GeV}^2$ are compared in Fig. 2a, which shows the valence quark distributions xu_v and xd_v, together with the gluon (xg) and sea (xS) quark densities both scaled down by a factor of 20. The two results are consistent at the 5 to 10% level and also agree with the results from global analyses as can be seen from the comparison in Fig. 2b. This is remarkable in view of the different methods and the different data sets used. Compared to the ZEUS results the systematic uncertainty of the H1 PDFs are, however, clearly larger. This is expected as in H1 PDF 2000 fit only H1 data are used, which have limited sensitivity to the valence quark distributions. When including the BCDMS data the uncertainties on the H1 result are substantially reduced.

In the central H1 and ZEUS fits, α_s is kept fixed. If treated as a free parameter ZEUS obtains $\alpha_s(M_Z^2) = 0.1166 \pm 0.0052$ [13], with an additional renor-

malization scale uncertainty of ± 0.004. This is in agreement with an earlier dedicated H1 analysis yielding $\alpha_s(M_Z^2) = 0.1166^{+0.0019}_{-0.0018} \pm 0.005$ [3], where the second error contribution is again estimated by varying the renormalization scale. This latter uncertainty is expected to be considerably reduced by full NNLO calculations expected to be completed soon [17].

2.2 The Longitudinal Structure Function F_L

In the one-photon exchange approximation, which is applicable for Q^2-values up to $Q^2 \approx 1000$ GeV^2, the deep-inelastic scattering cross section given in equation (1) reduces to

$$\frac{d^2\sigma}{dx\,dQ^2} = \frac{2\pi\alpha^2}{xQ^4}\left(Y_+\,F_2(x,Q^2) - y^2 F_L(x,Q^2)\right) \quad , \tag{6}$$

with F_2 and F_L representing the electromagnetic (γ–exchange only) contribution to $\mathcal{F}_2$ and $\mathcal{F}_L$. An extraction of the longitudinal structure function F_L is therefore only possible at high values of y, where the F_L–contribution becomes significant. In order to disentangle the contributions from F_2 and F_L in a model independent manner, measurements of $d^2\sigma/dx\,dQ^2$ at fixed x and Q^2 for different values of y are necessary. A direct measurement of F_L thus requires ep–scattering data at different center-of-mass energies, which up to now are not available at HERA[2].

An indirect determination of F_L is, however, possible using DIS cross section measurements at high values of y. Several extraction methods have been developed by the H1 collaboration [3, 18] all of which make use of the different behaviour of the reduced measured cross section $\sigma_r = \frac{d^2\sigma}{dx\,dQ^2}\frac{xQ^4}{2\pi\alpha^2 Y_+} = F_2 - \frac{y^2}{Y_+}F_L$, and the structure function F_2, which is extrapolated to high y using low–y data. Fig. 3a shows the Q^2 dependence of the longitudinal structure function F_L at fixed $y \approx 0.75$ and summarizes all F_L values extracted by H1 using these methods. The data points are in good agreement with most of the theoretical predictions [19, 20] shown; at low Q^2 the MRST 2001 parametrization [15] is disfavoured. Concerning the H1 QCD fit note that it is quoted not to be applicable in the region below $Q^2 = 1$ GeV^2 [3].

ZEUS has recently presented the first direct HERA measurement of F_L using initial state radiative (ISR) events [21]. For these events the center-of-mass energy of the ep–reaction is reduced due to emission of a hard photon off the initial state electron. The result is shown in Fig. 3b. Although the measurement is not very precise, it is clearly consistent with the expectations from perturbative QCD.

[2]The difference in the center-of-mass energy due to the change in the proton beam energy from 820 to 920 GeV is not sufficient for a measurement of F_L at HERA.

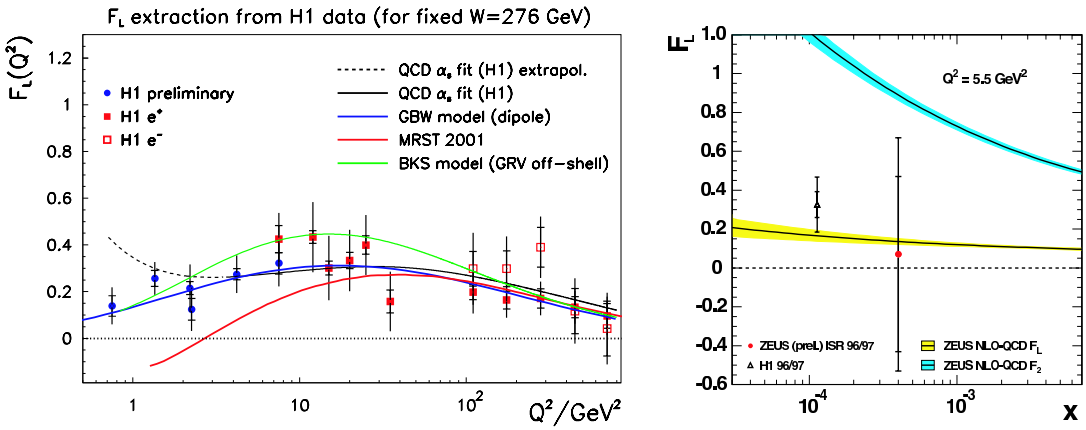

Figure 3: *(a) The Q^2 dependence of the longitudinal structure function F_L at fixed $y \approx 0.75$ ($W = 276$ GeV $\approx \sqrt{ys}$), summarizing the F_L values extracted from H1 cross section measurements [3, 6, 18]. (b) Direct F_L–measurement at $x = 4 \cdot 10^{-4}$ and $Q^2 = 5.5$ GeV^2 extracted from ZEUS ISR data [21].*

2.3 The Measurement of xF_3

The difference between the e^-p and the e^+p NC cross sections can be used to extract the generalized structure function $x\mathcal{F}_3$ and — since at HERA the dominant contribution to $x\mathcal{F}_3$ comes from the γZ–interference — to evaluate the structure function $xF_3^{\gamma Z}$, which is more closely related to the quark structure of the proton. Fig. 4a shows the $x\mathcal{F}_3$ x-dependence as measured by the H1 and ZEUS experiments [4, 9] in six different bins of Q^2. Here, $x\mathcal{F}_3$ is obtained from[3]

$$x\mathcal{F}_3 = \frac{1}{2Y_-}\left[\tilde{\sigma}^-_{\rm NC} - \tilde{\sigma}^+_{\rm NC}\right] \tag{7}$$

where the contribution of $\mathcal{F}_L$ can again be neglected; $\tilde{\sigma}^-_{\rm NC}$ and $\tilde{\sigma}^+_{\rm NC}$ represent the reduced neutral current cross sections obtained from (1) by removing the trivial $2\pi\alpha^2/xQ^4$ dependence. The results are in good agreement with the QCD prediction.

From these data H1 and ZEUS extract [4,9] the structure function $xF_3^{\gamma Z} = 2e_q a_q\,[q - \bar{q}]$ dividing $x\mathcal{F}_3$ by the factor $-a_e\kappa_w Q^2/(Q^2 + M_Z^2)$; remaining contributions arising from pure Z-exchange are estimated to be less than 3% and hence neglected. Fig. 4b shows $xF_3^{\gamma Z}$ as a function of x for Q^2=1500 GeV^2.

The presented measurement yields first direct information on the valence quark content of the proton at high Q^2. It is consistent with zero at large x rising to a maximum at $x \approx 0.1$. To quantify the level of agreement between data and

[3]If data at different center-of-mass energies are used the expression has to be modified slightly.

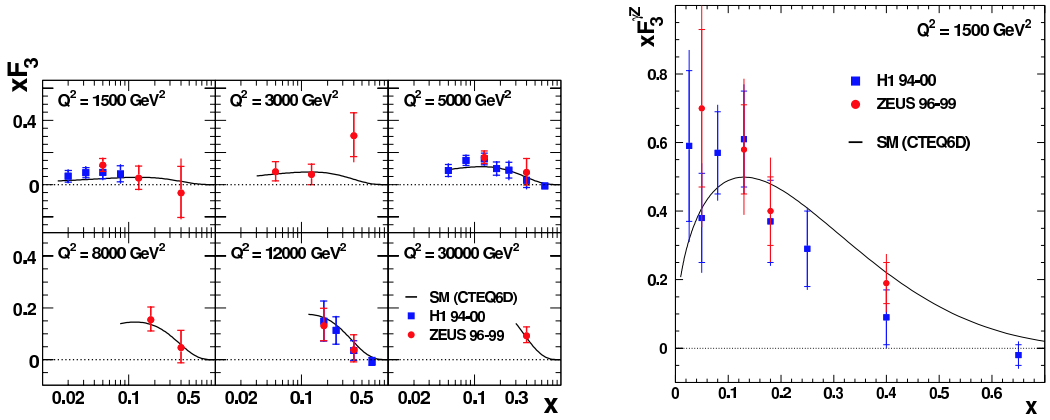

Figure 4: *(a) The generalized structure function $x\mathcal{F}_3$, as extracted by H1 and ZEUS. The data are plotted at fixed Q^2 as a function of x. (b) Structure function $xF_3^{\gamma Z}$ as a function of x at Q^2=1500 GeV^2. All data are compared to predictions based on the CTEQ6D parametrization [16] of the proton PDFs. Inner error bars represent the statistical, outer error bars the total error.*

theory the following sum rule has been formulated [22] in analogy to the Gross Llewellyn-Smith sum rule [23]: $\int_0^1 F_3^{\gamma Z} dx \approx 5/3$. Using the H1 data integration yields $\int_{.02}^{.65} = 1.28 \pm 0.20$. The corresponding integral obtained for the H1 PDF fit gives 1.06 ± 0.02 in agreement with the measured value.

3 Jet Physics

Jet production in electron-proton collisions at HERA provides a unique testing ground for Quantum Chromodynamics (QCD). Apart from the determination of the strong coupling constant α_s, ep jet data at large transverse momenta, E_T, may especially be used to gain insight into the dynamics of the exchanged parton cascade, whose structure is probed by the high-E_T dijet system.

3.1 α_s Determination

Jet production at large Q^2 and large E_T has been intensively studied by both the H1 and the ZEUS collaboration. In this region pertrubative QCD holds such that it is possible to determine the strong coupling constant α_s. The renormalization scale μ_r^2 at which α_s is determined is given, depending on the process studied, by either Q^2 or E_T^2.

Fig 5a shows one of the most recent α_s measurements [24] determined from jet production in γp interactions ($Q^2 \approx 0$); α_s is shown as a function of $\mu_r = E_T$ clearly revealing the expected scale dependence of the strong coupling.

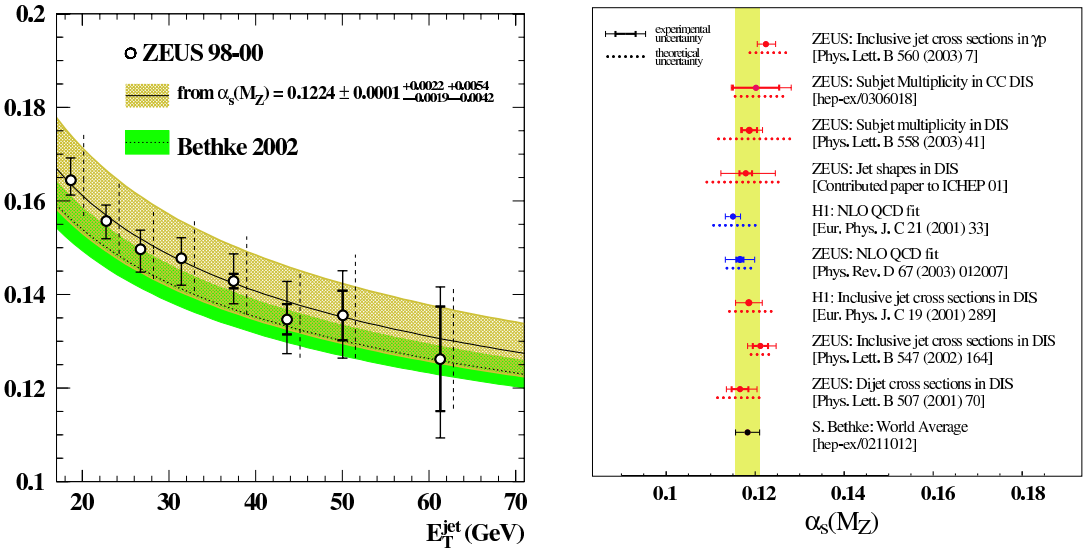

Figure 5: *(a) The $\alpha_s(E_T)$ values determined from a QCD fit to the differential γp cross section $d\sigma/dE_T$ in different E_T regions (open circles). The solid line represents the prediction of the renormalization group equation obtained from the $\alpha_s(M_Z)$ central value as determined in the analysis; the light-shaded area displays its uncertainty. (b) Summary of HERA α_s measurements in comparison to world average [25].*

When evolved to the mass of the Z–boson the analysis yields

$$\alpha_s(M_Z) = 0.1224 \pm 0.0001\ (\text{stat.})^{+0.0022}_{-0.0042}\ (\text{exp.})^{+0.0054}_{-0.0042}\ (\text{theo.})$$

in agreement with the world average [25] and other α_s-measurements performed at HERA, summarized in Fig. 5b. Concerning the experimental uncertainty this value is presently the most precise measurement of α_s from jets in ep–scattering.

3.2 Probing Parton Dynamics

HERA jet data cover a large range of Q^2, Bjorken-x and the transverse energy, E_T, of the observed jets. At low x, HERA dijet data may be used to gain insight into the dynamics of the parton cascade typically exchanged in low-x lepton-proton interactions.

Special insight into small-x dynamics can be gained from inclusive dijet data by studying the behavior of events with a small azimuthal separation, $\Delta\phi^*$, between the two hardest jets as measured in the hadronic center-of-mass system [26,27]. Partons entering the hard scattering process with negligible transverse momentum, k_t, as assumed in the DGLAP formalism [12], lead at leading order to a back-to-back configuration of the two outgoing jets with $\Delta\phi^* \sim 180°$. Azimuthal jet separations

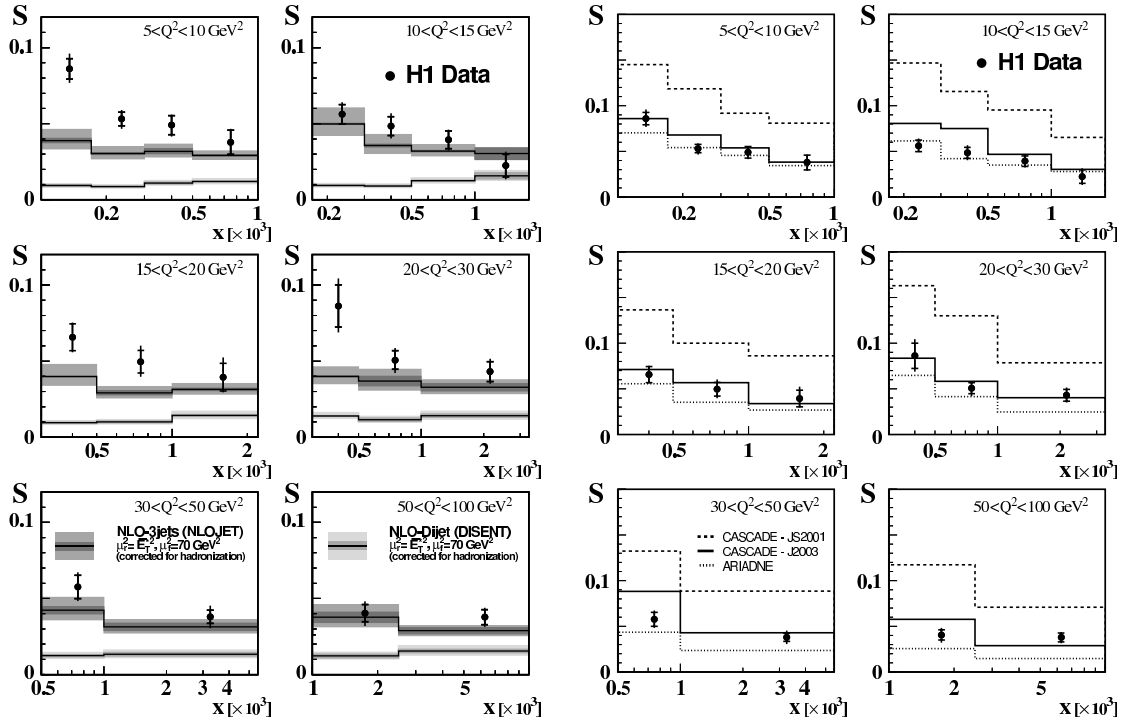

Figure 6: *Ratio S of events with small azimuthal separation ($\Delta\phi^*<120°$) of the two most energetic jets with respect to the total number of inclusive dijet events given as a function of Bjorken-x and Q^2 [30]. (a) H1 data in comparison to NLO-dijet and 3-jet calculations. (b) H1 data in comparison to predictions from ARIADNE and CASCADE.*

different from 180° occur due to higher order QCD effects. However, in models which predict a significant proportion of partons entering the hard process with large k_t, the number of events with small $\Delta\phi^*$ should increase. This is the case for the BFKL [28] and CCFM [29] evolution schemes.

The H1 collaboration has studied the ratio S [30] of the number of events N_{dijet} with an azimuthal jet separation of $\Delta\phi^* < \alpha$ relative to all dijet events as proposed in [27]. Fig 6 shows the S distribution for $\alpha = 120°$ as a function of x and Q^2. For the chosen α the measured values of S are of the order of 5%. NLO dijet QCD calculations [31] predict much too low S-values. The additional hard emission, provided by the NLO 3-jet calculation [32] considerably improves the description of the data, but is insufficient at low x and low Q^2. A similar description of the data is provided by RAPGAP [33] a DGLAP-based QCD model, which matches LO matrix elements for direct and resolved processes to k_t-ordered parton cascades (not shown). A good description of the measured ratio S is given by the ARIADNE program [34], which generates non-k_t-ordered parton cascades using the color dipole model [35].

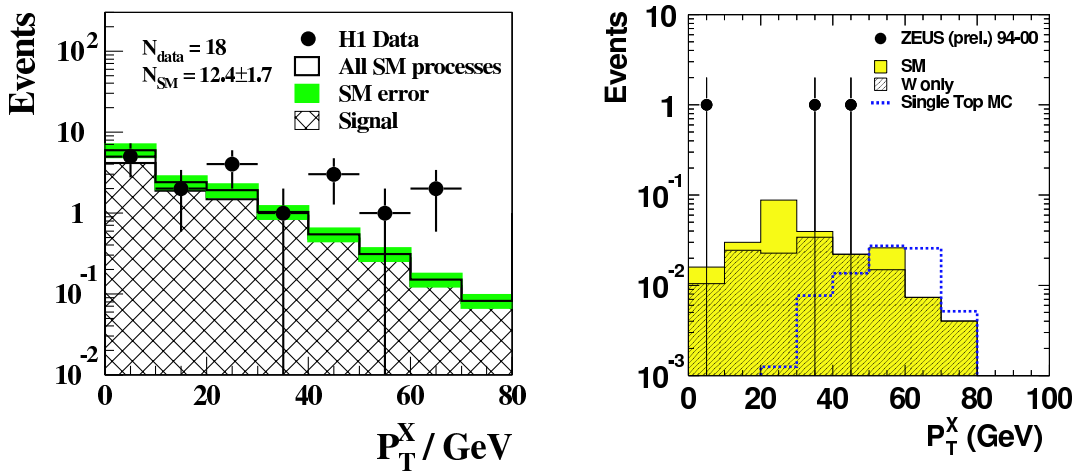

Figure 7: *Event distribution for events with missing transverse momentum and an isolated electron/muon (a) or and isolated tau (b) as a function of P_T^X, the transverse momentum of the recoiling hadronic system.*

Predictions based on the CCFM evolution equations and k_t factorized unintegrated gluon densities are provided by the CASCADE Monte Carlo program [36]. Large differences are found between the predictions for two different choices of the unintegrated gluon density, both of them describing the H1 structure function, and one of them giving a good description of S. This measurement thus provides a significant constraint on the unintegrated gluon density.

4 Search for Exotic Final States with Leptons

By investigating very hard processes in ep–scattering H1 and ZEUS have searched for phenomena beyond the Standard Model ($\mathcal{SM}$) resulting in a variety of constraints on models involving leptoquarks, supersymmetry, excited fermions, large extra dimensions etc. Deviations from the $\mathcal{SM}$-expectation have been found for two very distinct signatures: high energy isolated leptons in events with missing transverse momentum [37–39] and multi-electron events [40]. Concerning the first signature, the H1 collaboration has reported [37] an excess in the electron and muon channels. For P_T^X>40 GeV, where P_T^X is the transverse momentum of the recoiling hadronic system, H1 observes 3 (3) events in the electron (muon) channel with 0.54 ± 0.11 (0.55 ± 0.12) expected from the $\mathcal{SM}$ mainly due to production of W-Bosons. No such events are observed in a similar analysis by ZEUS with $0.94^{+0.11}_{-0.10}$ ($0.95^{+0.11}_{-0.10}$) expected [38]. However, as preliminary result [39] ZEUS finds two events in the tau channel for P_T^X>25 GeV, where only 0.12 ± 0.02 are predicted by the $\mathcal{SM}$. Fig. 7

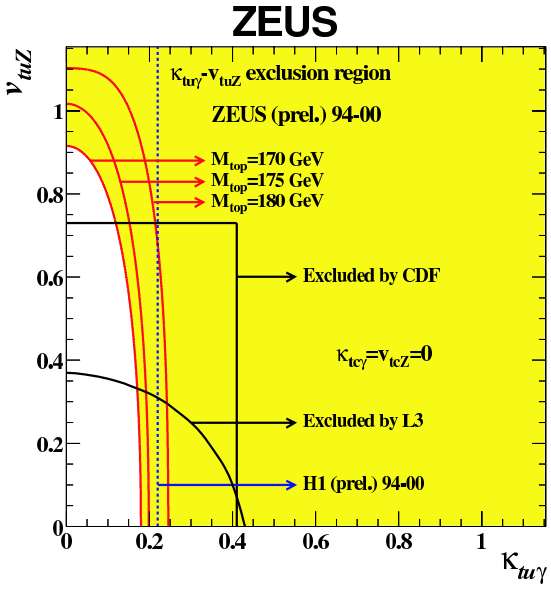

Figure 8: *ZEUS exclusion regions at 95% CL in the $\kappa_{tu\gamma}$-v_{tuZ} plane for three values of M_{top} assuming $\kappa_{tc\gamma} = v_{tcZ} = 0$. Exclusion limits from H1, CDF and L4 are also shown.*

shows the corresponding event distribution for electrons and muons (taus) observed by H1 (ZEUS) as a function of P_T^X.

One possible explanation for the observed isolated lepton events is anomalous single-top production, $ep \to etX$, via flavour changing neutral currents (FCNC). The anomalous couplings to the photon and the Z–boson, $tu\gamma$ and tuZ, are parametrized by the magnetic coupling $\kappa_{tu\gamma}$ and the vector coupling v_{tuZ}. Both collaborations have performed dedicated searches for such processes considering both leptonic and hadronic decays of the produced top. The H1 experiment sees several candidate events, a subset of the isolated electron and muon events with missing transverse momentum. Exclusion limits on $\kappa_{tu\gamma}$ and v_{tuZ} from HERA [38,41] as well as CDF [42] and L3 [43] are summarized in Fig 8.

Concerning the multi-electron signature, H1 has reported [40] an excess of three clean di-electron and three clean tri-electron events with an invariant di-lepton mass, M_{12}, of the two electrons with highest transverse momentum above 100 GeV; the corresponding $\mathcal{SM}$ expectations are 0.30 ± 0.004 and 0.23 ± 0.04, respectively. A similar and still preliminary analysis performed by ZEUS [39] reveals two di-electron and no tri-electron event, with 0.77 ± 0.08 and 0.37 ± 0.04 expected.

5 Summary

Some of the most recent results obtained analyzing hard process in ep–interactions have been presented. From inclusive deep-inelastic scattering (DIS) data insight into the dynamic structure of the proton is gained yielding information on the proton

parton content and the strong coupling constant α_s. Measurements of ep jet cross sections provide important tests of perturbative QCD; by analyzing various aspects of jet data several values of α_s are obtained all in agreement with each other, the result from inclusive DIS data and the world average. Some new insight into small-x dynamics is gained by a very recent result, obtained studying dijet events with small separation in azimuth of the two most energetic jets. In general, by investigating hard processes in ep–interactions many aspects of the Standard Model can be tested. Any observed deviation between the data and existing theoretical models could hint at signs of new physics. Two such deviations have been observed at HERA when searching for events with a high-p_t isolated lepton and missing transverse momentum and multi-electron topologies.

6 Acknowledgements

This work was supported by the Bundesministerium für Bildung, Wissenschaft, Forschung und Technologie, Germany (contract no. 05H11PEA/6).

References

1. E. Derman, Phys. Rev. D **7** (1973) 2755.
2. G. Ingelman and R. Rückl, Phys. Lett. B **201** (1988) 369.
3. C. Adloff *et al.* [H1 Collaboration], Eur. Phys. J. C **21** (2001) 33.
4. C. Adloff *et al.* [H1 Collaboration], Eur. Phys. J. C **19** (2001) 269.
5. C. Adloff *et al.* [H1 Collaboration], DESY-03-038, submitted to Eur. Phys. J. C.
6. H1 Collaboration, contributed paper 799, EPS 2001, Budapest.
7. H1 Collaboration, contributed paper 082, EPS 2003, Aachen.
8. S. Chekanov *et al.* [ZEUS Collaboration], Eur. Phys. J. C **21** (2001) 443.
9. S. Chekanov *et al.* [ZEUS Collaboration], Eur. Phys. J. C **28** (2003) 175.
10. S. Chekanov *et al.* [ZEUS Collaboration], Phys. Lett. B **539** (2002) 197 [Erratum-ibid. B **552** (2003) 308].
11. S. Chekanov *et al.* [ZEUS Collaboration], DESY-03-093, submitted to Eur. Phys. J. C.

12. V. Gribov, L.N. Lipatov, Sov. J. Nucl. Phys. **15** (1972) 438 and 675; L.N. Lipatov, Sov. J. Nucl. Phys.**20** (1975) 94; G. Altarelli and G. Parisi, Nucl. Phys. B **126** (1977) 298; Y.L. Dokshitzer, Sov. Phys. JETP **46** (1977) 641.

13. S. Chekanov *et al.* [ZEUS Collaboration], Phys. Rev. D **67** (2003) 012007.

14. W. Furmanski and R. Petronzio, Phys. Lett. B **97** (1980) 437.

15. A. D. Martin, R. G. Roberts, W. J. Stirling and R. S. Thorne, Eur. Phys. J. C **23** (2002) 73.

16. J. Pumplin, D. R. Stump, J. Huston, H. L. Lai, P. Nadolsky and W. K. Tung, JHEP **0207** (2002) 012.

17. S. Moch, J. A. Vermaseren and A. Vogt, Nucl. Phys. B **646** (2002) 181.

18. H1 Collaboration, contributed paper 083, EPS 2003, Aachen.

19. K. Golec-Biernat and M. Wusthoff, Phys. Rev. D **59** (1999) 014017.

20. B. Badelek, J. Kwiecinski and A. Stasto, Z. Phys. C **74** (1997) 297.

21. ZEUS Collaboration, contributed paper 502, EPS 2003, Aachen.

22. E. Rizvi and T. Sloan, Eur. Phys. J. directC **3** (2001) N2.

23. D. J. Gross and C. H. Llewellyn Smith, Nucl. Phys. B **14** (1969) 337.

24. S. Chekanov *et al.* [ZEUS Collaboration], Phys. Lett. B **560** (2003) 7.

25. S. Bethke, arXiv:hep-ex/0211012.

26. J. R. Forshaw and R. G. Roberts, Phys. Lett. B **335** (1994) 494; J. Kwiecinski, A. D. Martin and A. M. Stasto, Phys. Lett. B **459** (1999) 644; A. J. Askew, D. Graudenz, J. Kwiecinski and A. D. Martin, Phys. Lett. B **338** (1994) 92.

27. A. Szczurek, N. N. Nikolaev, W. Schafer and J. Speth, Phys. Lett. B **500** (2001) 254.

28. V.S. Fadin, E.A. Kuraev and L.N. Lipatov, Sov. Phys. JETP **44** (1976) 443; V.S. Fadin, E.A. Kuraev and L.N. Lipatov, Sov. Phys. JETP **45** (1977) 199; Y. Balitsky and L.N. Lipatov, Sov. J. Nucl. Phys. **28** (1978) 822.

29. M. Ciafaloni, Nucl. Phys. B **296** (1988) 49; S. Catani, F. Fiorani and G. Marchesini, Phys. Lett. B **234** (1990) 339; S. Catani, F. Fiorani and G. Marchesini, Nucl. Phys. B **336** (1990) 18; G. Marchesini, Nucl. Phys. B **445** (1995) 49.

30. A. Aktas *et al.* [H1 Collaboration], DESY-03-160 to be submitted to Eur. Phys. J. C.

31. S. Catani and M.H. Seymour, Nucl. Phys. B **485** (1997) 291 [Erratum-ibid. B **510** (1997) 503].

32. Z. Nagy and Z. Trocsanyi, Phys. Rev. Lett. **87** (2001) 082001.

33. H. Jung, Comp. PhysĊommun. **86** (1995) 147; H. Jung, *The RAPGAP Monte Carlo for Deep Inelastic Scattering, version 2.08*, Lund University, 1999.

34. L. Lönnblad, Comp. Phys. Commun. **71** (1992) 15.

35. B. Andersson, G. Gustafsson and L. Lönnblad, Nucl. Phys. B **339** (1990) 393.

36. H. Jung and G. Salam, Eur. Phys. J. C **19** (2001) 351; H. Jung, Comp. Phys. Commun. **143** (2002) 100.

37. V. Andreev *et al.* [H1 Collaboration], Phys. Lett. B **561** (2003) 241.

38. S. Chekanov *et al.* [ZEUS Collaboration], Phys. Lett. B **559** (2003) 153.

39. ZEUS Collaboration, contributed paper 909, ICHEP 2002, Amsterdam.

40. A. Aktas *et al.* [H1 Collaboration], DESY-03-082, submitted to Eur. Phys. J. C.

41. H1 Collaboration, contributed paper 100, EPS 2003, Aachen.

42. F. Abe *et al.* [CDF Collaboration], Phys. Rev. Lett. **80** (1998) 2525; V. F. Obraztsov, S. R. Slabospitsky and O. P. Yushchenko, Phys. Lett. B **426** (1998) 393.

43. P. Achard *et al.* [L3 Collaboration], Phys. Lett. B **549** (2002) 290.